

PROCEEDINGS OF SPIE

[SPIEDigitallibrary.org/conference-proceedings-of-spie](https://www.spiedigitallibrary.org/conference-proceedings-of-spie)

High surface area reverse electrowetting energy harvesting with power conditioning circuitry for self-powered motion sensors

Adhikari, Pashupati, Biswas, Dipon, Tasneem, Nishat, Reid, Russell, Mahbub, Ifana

Pashupati R. Adhikari, Dipon K. Biswas, Nishat T. Tasneem, Russell C. Reid, Ifana Mahbub, "High surface area reverse electrowetting energy harvesting with power conditioning circuitry for self-powered motion sensors," Proc. SPIE 11722, Energy Harvesting and Storage: Materials, Devices, and Applications XI, 117220T (12 April 2021); doi: 10.1117/12.2587541

SPIE.

Event: SPIE Defense + Commercial Sensing, 2021, Online Only

High surface area reverse electrowetting energy harvesting with power conditioning circuitry for self-powered motion sensors

Pashupati R. Adhikari^a, Dipon K. Biswas^b, Nishat T. Tasneem^b, Russell C. Reid^c, Ifana Mahbub^b

^aDepartment of Mechanical Engineering; University of North Texas, Denton, TX USA 76207

^bDepartment of Electrical Engineering; University of North Texas, Denton, TX USA 76207

^cDepartment of Mechanical Engineering; Dixie State University, St. George, UT USA 84770

ABSTRACT

Monitoring human health in real-time using wearable and implantable electronics (WIE) has become one of the most promising and rapidly growing technologies in the healthcare industry. In general, these electronics are powered by batteries that require periodic replacement and maintenance over their lifetime. To prolong the operation of these electronics, they should have zero post-installation maintenance. On this front, various energy harvesting technologies to generate electrical energy from ambient energy sources have been researched. Many energy harvesters currently available are limited by their power output and energy densities. With the miniaturization of wearable and implantable electronics, the size of the harvesters must be miniaturized accordingly in order to increase the energy density of the harvesters. Additionally, many of the energy harvesters also suffer from limited operational parameters such as resonance frequency and variable input signals. In this work, low frequency motion energy harvesting based on reverse electrowetting-on-dielectric (REWOD) is examined using perforated high surface area electrodes with 38 μm pore diameters. Total available surface area per planar area was 8.36 cm^2 showing a significant surface area enhancement from planar to porous electrodes and proportional increase in AC voltage density from our previous work. In REWOD energy harvesting, high surface area electrodes significantly increase the capacitance and hence the power density. An AC peak-to-peak voltage generation from the electrode in the range from 1.57-3.32 V for the given frequency range of 1-5 Hz with 0.5 Hz step is demonstrated. In addition, the unconditioned power generated from the harvester is converted to a DC power using a commercial off-the-shelf Schottky diode-based voltage multiplier and low dropout regulator (LDO) such that the sensors that use this technology could be fully self-powered. The produced charge is then converted to a proportional voltage by using a commercial charge amplifier to record the features of the motion activities. A transceiver radio is also used to transmit the digitized data from the amplifier and the built-in analog-to-digital converter (ADC) in the micro-controller. This paper proposes the energy harvester acting as a self-powered motion sensor for different physical activities for wearable and wireless healthcare devices.

Keywords: Energy harvesting, Reverse electrowetting, Charge amplifier, Voltage multiplier, Low dropout regulator.

1. INTRODUCTION

Remote health monitoring in real-time using wearable and implantable electronics (WIE) has become one of the most promising and rapidly growing technologies in the healthcare industry.^{1, 2, 3} Often powered by battery, these remote health monitoring electronics can be much more reliable and cost effective if the primary source of the power, the batteries, are replaced by an energy harvesting system that can harvest energy from various human motion activities such as walking, running, jogging, and several other physical activities. Batteries not only occupy most of the space in the electronics, but also add significant weight and cause safety issues due to possible electrolyte leakage that is flammable in nature. Collectively, these issues also go against the portability of the wearables.⁴ Although significant progress has been made in increasing the capacity of the batteries and reducing the power consumption of the devices, these systems still need rigid batteries with frequent replacement or charging process, which greatly limits their application and brings inconvenience to the user. Therefore, there is an urgent need to develop an energy harvesting system that can consistently and sufficiently generate power without any external bias source and operate solely based on the energy harvested from human motion activities. As a result, this will help improve the longevity and reliability of these electronics for human health monitoring.

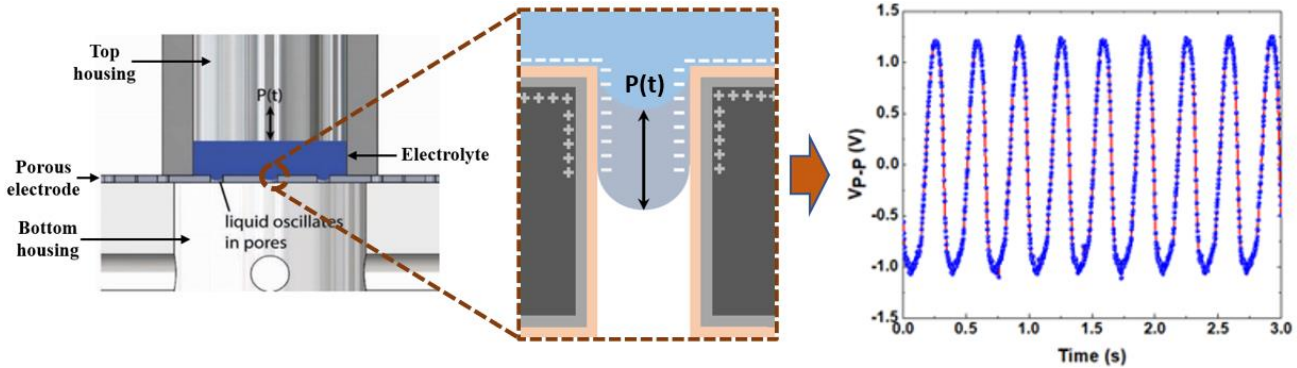


Figure 1. High surface area REWOD energy harvesting configuration used for this study. Pulsating pressure, $P(t)$, is applied to insert and retract liquid electrolyte in and out of the pores.

Various well established energy harvesting technologies have emerged over the years such as vibrational, thermoelectric, piezoelectric, and electromagnetic energy harvesting.^{5, 6, 7, 8} While these technologies have received significant attention in research and are reliably used for specific applications, most, if not all, fail to harvest energy at lower frequency range (<5 Hz) with high power density. In addition, these energy harvesting technologies require resonance of solid structures to operate, which is typically over 30 Hz, making them quite unsuitable for harvesting energy from human motion-related activities. Based on the limitations of the existing energy harvesting technologies, energy harvesting based on reverse electrowetting-on-dielectric (REWOD) has been developed within the last decade.⁹ REWOD has been shown to operate efficiently at the typical frequency range of human motion (1-5 Hz).¹⁰ REWOD is opposite to electrowetting-on-dielectric (EWOD) in which an electric field applied to an electrolyte modifies the effective surface tension and produces electrolyte movement.¹¹ In REWOD, applied mechanical modulation changes electrolyte displacement and thereby changes the electrode-electrolyte interfacial area, resulting in a periodic variation in capacitance. Due to the variation in capacitance, charges are drawn towards or discharged from the interface, and a voltage difference across the electrodes is realized. This mechanism is equivalent to a variable capacitor such that the energy harvested using REWOD is directly proportional to the interfacial capacitance. Prior research in REWOD have solely relied on planar electrodes which by its geometry has a fixed interfacial area, limiting capacitance and hence power density output.^{12, 13, 14,}¹⁵ In order to enhance the power density from REWOD energy harvesting, this work presents a mechanism to increase the surface area of the electrodes by perforating Si wafers with numerous micro-sized pores. This essentially creates a much higher surface area per planar area resulting in a much higher power density.

Figure 1 illustrates an example of the high surface area REWOD configuration wherein the porous electrode is coated with dielectric materials (SiO_2 and CYTOP). A conductive electrolyte is inserted and retracted in and out of the pores under the application of a time varying pulsating pressure, $P(t)$, thereby periodically modulating electrical capacitance and hence generating an AC voltage across the electrodes. The formation of electrical capacitance is due to the capacitance from the electrical double layer (EDL) at the solid-liquid interface and across the dielectric insulator. EDL capacitance is typically neglected because when combined in series with the dielectric layer capacitance, the EDL capacitance is negligible. The capacitance can be modeled as given in Equation 1.

$$C = \frac{\epsilon_0 \epsilon_r A}{d} \quad (1)$$

where $\epsilon_0 = 8.85 \times 10^{-12} \text{ F/m}$ is the vacuum permittivity, ϵ_r is the relative permittivity of the dielectric material, A is the electrode-electrolyte interfacial area, and d is the thickness of the dielectric layer. Among all the parameters influencing the capacitance, electrode-electrolyte interfacial area plays the most dominant role in maximizing the capacitance and hence the output voltage.

High surface area electrodes that possess much higher surface area as compared to its planar area are ideal for REWOD energy harvester that could be integrated to power WIEs, which have become significantly miniaturized over the years.^{16, 17} With respect to powering miniaturized WIEs, power density, which is the power generated per unit area (W/cm^2), is one of the most important parameters to consider in REWOD energy harvesting. While high surface area electrodes

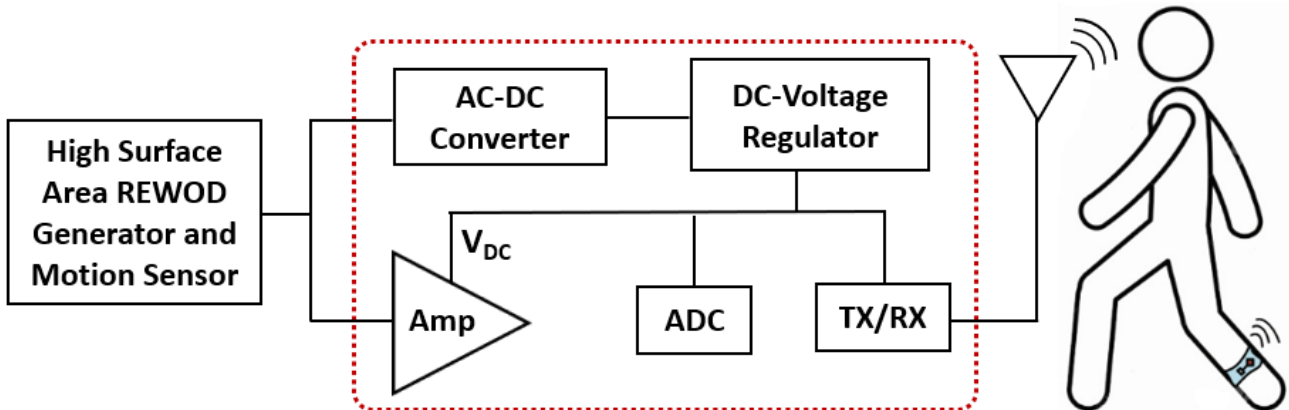


Figure 2. The block-level diagram of REWOD based self-powered motion sensor integrated with charge amplifier and DC-DC converter.

significantly enhance power output compared to planar electrodes, the absence of bias voltage could make the WIEs fully self-powered. In such a scenario, the voltage generated from the REWOD as an input could be rectified to convert the AC signal to a DC voltage and then boosted and regulated to supply a constant DC power by using a DC-DC converter.¹⁸ All of these components could be integrated within the WIEs and hence power the device without requiring an external voltage source and also contributing to miniaturization of the device. To the best of the authors' knowledge, very few works have been published where the energy harvester is integrated with a rectifying circuit and is able to self-power analog circuits. The most challenging part of designing a rectification circuit is to make the system operate at a very low frequency range. A commercially available power management unit has been used for low frequency energy scavenging.¹⁹ However, the proposed system works at 7.8 Hz frequency. As the REWOD energy harvester works in the frequency range of 1-5 Hz, a rectification circuit that operates in the same frequency range needs to be designed to make the sensor self-powered. As shown in Figure 2, a rectifier circuit followed by voltage regulator circuit can be used to convert the harvested AC voltage to a constant DC voltage to power up the other analog circuitry such as amplifier, analog-to-digital converter (ADC), and transceiver (TX/RX).

Since REWOD can transduce the mechanical modulation between the two electrodes into an electric current, it would be a good fit for motion sensing applications. Several movement and activity tracking sensors are proposed in the literature, such as accelerometers and pedometers.²⁰ Even though these devices measure human physical activities, they exhibit the shortfalls of storing long-term data and requiring a battery. In this work, we propose a self-powered REWOD motion sensor, which would wirelessly send the movement data to a remote receiver. Figure 2 also depicts the REWOD harvester functioning as a motion tracking sensor, where the charge amplifier produces an output voltage proportional to the generated charge from the motion activities.^{21,22} Typically, the generated AC charge lacks the capability of distinguishing motion at various frequencies and displacements due to low resolution. Thus, transducing and amplifying the low amount of charge achieves improved signal-to-noise ratio (SNR) as well as high dynamic range for the motion sensor. Having the charge amplifier ensures an overall better resolution for the self-powered motion sensor. An ADC is also utilized in this work to digitize the amplified signal and finally a transceiver (TX/RX) transmits the data wirelessly to a remote receiver. In this work, REWOD harvester is not yet integrated with the power conditioning circuitry. As our future work, we envision a single unit in which both the REWOD energy harvester and motion sensor are integrated together as a single device.

2. EXPERIMENTAL SECTION

2.1 Electrode fabrication

A very low resistance (0.001 - 0.005 Ω -cm), 100 mm diameter, and 380 μ m thick double side polished silicon wafer (University Wafers Inc.) was used to fabricate the porous electrode with 38 μ m diameter uniform pores within a circular area of 3.14 cm^2 (1 cm radius). A high-resolution chrome mask was created from an AutoCAD generated DXF file for the

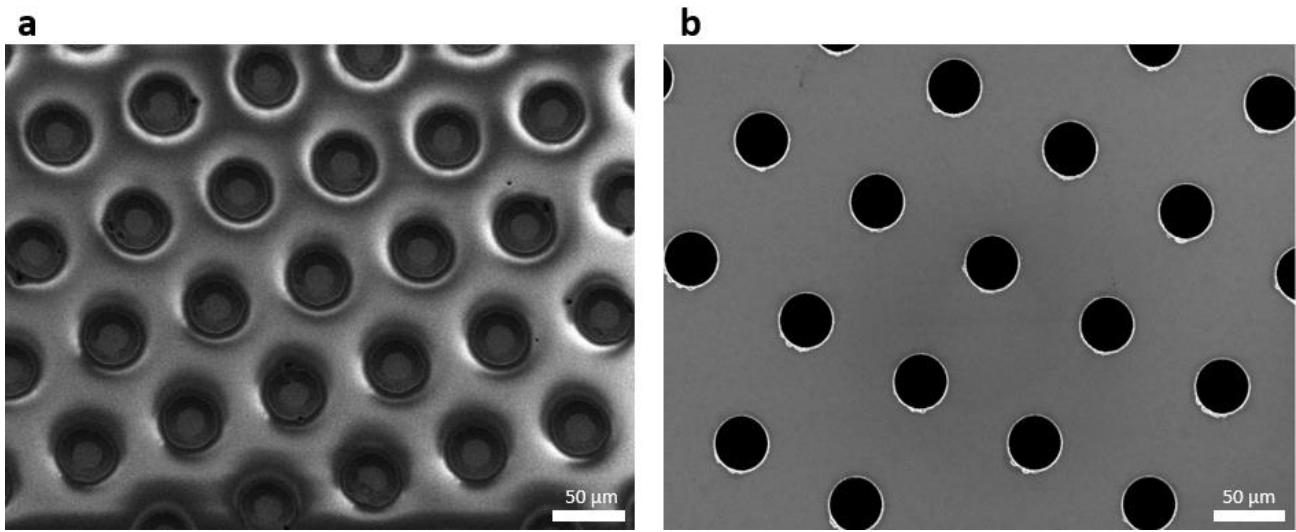


Figure 3. (a) Patterned photoresist on Si-wafer using photolithography with $\sim 10 \mu\text{m}$ thick positive photoresist, and (b) Etched holes using plasma deep reactive ion etching (DRIE).

given pore pattern. KL6008 positive photoresist (Kemlab Inc.) was spin coated on the wafer at 300 rpm for 5 seconds (spread cycle) and 600 rpm for 45 seconds (spin cycle). This process provided a sufficient photoresist thickness of $\sim 10\text{--}12 \mu\text{m}$ as required for safe deep reactive ion etching (DRIE) later in the fabrication process. Photoresist was cured for 150 seconds at 105°C on a hot plate. The cured wafer was then exposed under UV light for 45 seconds at 210 mJ/cm^2 of exposure broadband. Subsequently, the UV-exposed wafer was immediately developed using Tetramethylammonium Hydroxide, 0.26N (0.26N TMAH) developer for ~ 2 minutes, rinsed with deionized water, and nitrogen air dried. The pore patterns and the photoresist thickness on the developed wafer were verified using Alpha-Step D-300 Stylus Profiler (KLA Corporation). The patterned wafer was etched to create through pores using deep reactive ion etching (DRIE) (using Oxford 100 ICP) in the Nanofab facility at the University of Utah. The etched porous wafer was subjected to plasma CVD (Oxford Plasmalab 80) and deposited with SiO_2 dielectric. The anisotropic plasma DRIE was performed in the presence of sulfur hexafluoride (SF_6) at a flow rate of 80 sccm and Octafluorocyclobutane (C_4F_8) at a flow rate of 90 sccm under a vacuum pressure of $7.5 \mu\text{torr}$. Once etched, the wafers were thoroughly cleaned before CVD deposition of SiO_2 . Figure 3(a) shows a wafer patterned with photoresist using photolithography. A wafer with $38 \mu\text{m}$ diameter pores after DRIE and subsequent deposition of SiO_2 is shown in the accompanying Figure 3(b). Since the entire wafer was coated with SiO_2 during CVD and CYTOP dip coating, a small portion of the wafer was treated with hydrofluoric acid (HF) to remove the SiO_2 and CYTOP coating for an electrical connection to a wire lead.

2.2 Measurement Set-up

A custom-built measurement set-up for the high surface area REWOD energy harvesting is illustrated in Figure 4. A similar measurement set-up has been used in our prior REWOD works. It consists of a subwoofer generating pulsating pressure through a vertical displacement of a piston inside a syringe attached to it. The syringe is attached to a 3D printed stage over the subwoofer dust cap and only the piston is allowed to move in a vertical direction. The subwoofer is controlled by a signal generating application (Audio Function Generator PRO). This application works almost the same way as an actual function generator, except it excites the subwoofer in vertical mechanical displacement to a desired amplitude. The shaker system consists of an 8-inch 800-W subwoofer (Pyle), a 400 W amplifier (Boss CX250), and a 12-V power source (Apevia ATX Raptor) attached to a power adapter cord. Similar custom-made systems have been reported in prior energy harvesting research.^{23, 24} This was a simple, inexpensive method for generating low-frequency and relatively high amplitude oscillations. A custom wood enclosure provided a location to mount the subwoofer and also contained the amplifier and power source.

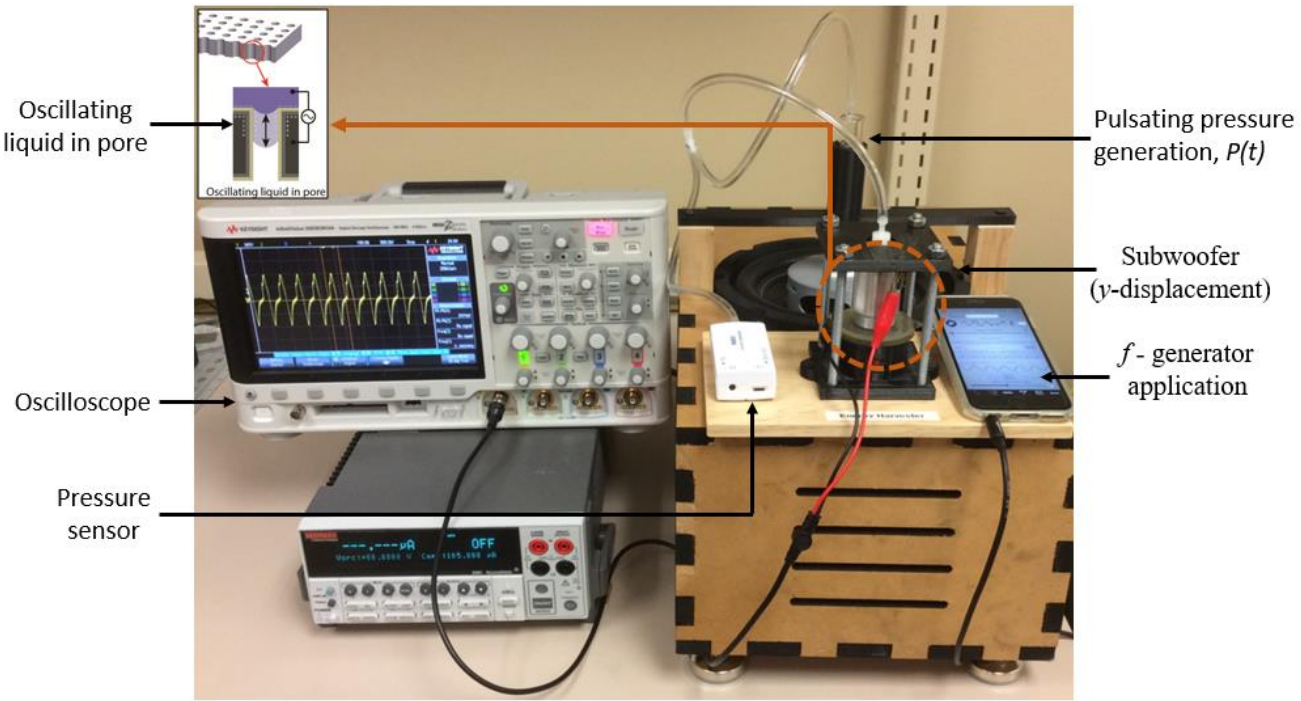


Figure 4. Measurement set-up of the high surface area REWOD energy harvesting. Application of pulsating pressure on the porous electrode with electrolyte on top of it, inside an air tight chamber is shown in the inset. Black and red cables from the oscilloscope connect to electrode and counter electrode, respectively.

The master volume feature in the mobile application corresponds to the amplitude of the vertical displacement of the syringe piston and hence the magnitude of the pressure generated. The pressure magnitude is higher for a higher frequency oscillation at a fixed master volume. Pressure can be precisely controlled as desired by adjusting the amplitude for any given frequency in the application. Pulsating pressure generated in the form of sinusoidal peak-to-peak pressure for a frequency range of 1-5 Hz with 1 Hz step size are measured using a pressure sensor (PASCO PS-320) and are approximately within the range of 1.5-16 kPa. This range of pressure is well within the range of Laplace capillary pressure required for the insertion and retraction of electrolyte in and out of the pores. The Laplace capillary pressure, as shown in Equation 2, is the pressure that is required for liquid to penetrate into the micropores.

$$P = \frac{2\gamma\cos\theta}{r} \quad (2)$$

where γ is the surface tension, θ is the contact angle, and r is the pore radius. The pressure that the subwoofer system is capable of generating straddles the Laplace capillary pressure. Once the pulsating pressure generated by the subwoofer system reaches the capillary pressure at a given frequency, the liquid electrolyte is inserted in and retracted out of the pores. This liquid movement results in a periodically changing electrode-electrolyte interfacial area resulting in a periodic change in charge, which produces an AC current.

Before the actual measurements of AC voltage began, several trial AC voltage measurements were performed by applying pulsating pressure in small increments starting with a lower limit (~1.5 kPa) to observe any increase in the magnitude of the AC voltage. In order to ensure that an optimum peak-to-peak pressure is identified such that there is neither excess pressure to cause electrolyte leakage from the porous electrode to the bottom chamber nor is there insufficient pressure inhibiting the electrolyte to cover the entire pore walls. Applied pressure from the pulsating pressure device was gradually increased to realize a proportional increase in the magnitude of the AC voltage until the AC signals disappeared from the oscilloscope indicating electrolyte leakage beneath the porous electrode. The pressure immediately before the lamented signal was adopted as the optimum peak-to-peak pressure. Theoretical capillary pressure as given by

the Laplace equation shown in Equation 2, where $\gamma = 0.072 \text{ N/m}$ and $\theta = 110^\circ$, was calculated for the given pore size.²⁵ The Laplace pressure for the $38 \mu\text{m}$ pore diameter electrode used in this work was determined to be 2.6 kPa and the corresponding experimental peak pressure was 2.8 kPa showing good agreement on pulsating pressure. The error percentage of 7.2, which is the difference between the theoretical and experimental peak pressure, could be attributed to a possible air pressure leakage during the experiment.

The REWOD energy harvesting unit in Figure 1 and also in the inset of Figure 4 consists of hollow upper and bottom chambers. The upper chamber is an aluminum housing and acts both as a counter electrode as well as an airtight compartment to prevent pressure leakage during experiment. The bottom housing is a 3D printed PLA fixture to support the electrode (the porous silicon wafer). The electrode is sealed on either side with silicone O-rings with the same circular area to that of the porous section of the electrodes (3.14 cm^2). Once the REWOD energy harvesting unit is secured, deionized water, which is used as an electrolyte in this work, is injected into the top housing to completely cover the porous area of the electrode. Then, AC voltage measurement is performed.

2.3 Motion sensor read-out circuit

A charge amplifier is used for converting the generated charge to a proportional output voltage. The schematic of the amplifier used for this research consists of a resistive-capacitive feedback network and is presented in Figure 5(a). Printed circuit board (PCB) of the read-out circuit is shown in Figure 5(b). The input impedance of the charge amplifier with the feedback network is designed in such a way to match the equivalent impedance of the REWOD transducer. The feedback resistor R_f is chosen to provide the DC path for the overall input currents of the operational transconductance amplifier (OTA). The value of R_f is $1 \text{ G}\Omega$ to achieve the high-pass frequency of 0.88 Hz . The input and the feedback capacitance values are chosen to be 470 pF and 180 pF , respectively, to achieve the gain of 8.33 dB (2.6 V/V), in the pass band. In this work, a general-purpose amplifier (model no: ADA4691-2) from Analog Devices is used as the charge amplifier.²⁶ The proportional output voltage from the amplifier (V_{out}) is digitized using the 12-bit ADC of CC430F5137.²⁷ This chip is a low-power microcontroller with the radio frequency (RF) transceiver integrated with it. The ADC uses an internal reference voltage of $V_{CC}/2$, where V_{CC} is the supply voltage of the transceiver (3.3V). The sampling frequency of the ADC is 0.45 MHz , which is set internally without using any external oscillator. The digitized signal is sent to a remote receiver through a ceramic antenna at 868 MHz with a transmission power of 0 dBm .

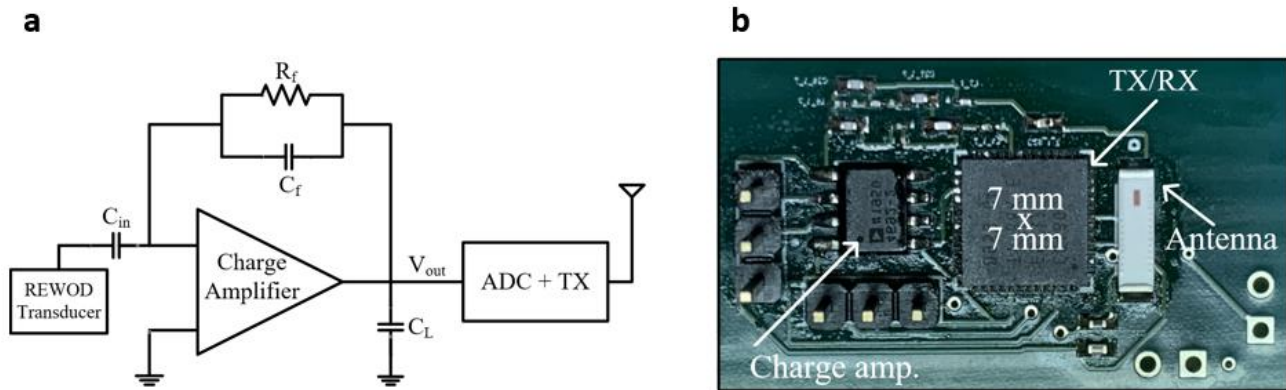


Figure 5. (a) Schematic of the proposed read-out circuit. (b) PCB of the read-out circuit.

2.4 Energy harvester

2.4.1 Voltage multiplier

The proposed voltage multiplier is a Schottky diode-based two-stage Cockcroft-Walton architecture.²⁸ A SC7630-079LF Schottky diode by Skyworks is used to design the voltage multiplier as shown in Figure 6(a). An image showing soldered PCB of the voltage multiplier is presented in Figure 6(b). During the negative cycle of the AC signal, the capacitor, C_1 is charged through the diode, D_1 and during the positive cycle of the AC signal, capacitor, C_2 is charged through diode,

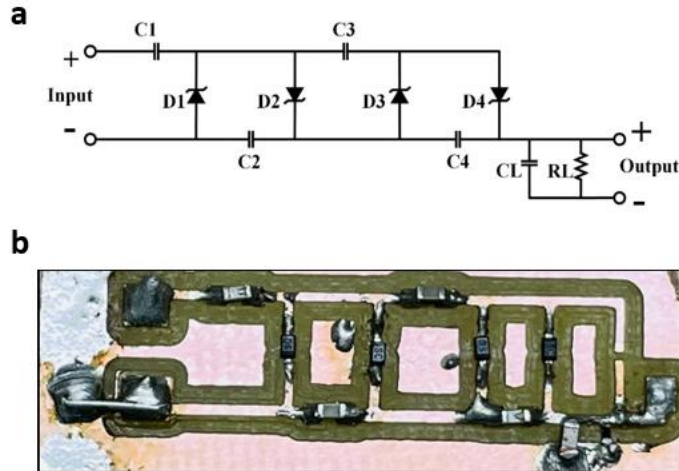


Figure 6. (a) Schematic of the voltage multiplier circuit. (b) Soldered PCB of the voltage multiplier.

D_2 . During the next negative half cycle, capacitor C_1 is discharged and allows the capacitor C_3 to be charged through the diode, D_3 . During the next positive half cycle, capacitor C_4 is charged through diode, D_4 . The output of the voltage multiplier is thus found to be the sum of the charges on C_2 and C_4 . For the low frequency applications of 1-10 Hz frequency range, the sizing of the capacitors is chosen to be 10 mF. A load capacitor, C_L , also of 10 mF is used to reduce the output ripples and a load resistance, R_L , of 11 k Ω is used to emulate the total load of the system. The value of the load resistor is calculated based on the voltage and current requirements of the charge-amplifier, which requires a 3.3 V supply voltage and 300 μ A current.

2.4.2 Low-dropout regulator

As the output of the voltage multiplier varies with the varying harvested energy by the REWOD system, a voltage regulator is needed to provide a constant voltage to the REWOD-based motion sensor read-out circuit. A TPS746-Q1 ultra low power low-dropout regulator (LDO) by Texas Instrument with high power supply rejection ratio (PSRR) of 38 dB is used to provide a constant voltage of 3.3 V.²⁹ The commercial LDO can provide a constant 3.3 V output when the nominal input voltage is higher than 3.3 V. The TPS746-Q1 has an input voltage range of 1.5 V to 6 V and an externally adjustable output voltage range of 0.55 V to 5.5 V. The commercial LDO is a WSON package with six pins as shown in Figure 7(a). PCB of the low dropout regulator is shown in Figure 7(b). The input capacitor, C_I with a value of 10 μ F, is used to improve the transient response, input ripple, and PSRR. If the input supply has a high impedance over a large frequency range, multiple capacitors can be used in parallel. An output capacitor, C_O also of 10 μ F, is used for stability. The output of the LDO is adjusted using a feedback resistive divider denoted by R_{FB} and R_{PG} . To achieve 3.3 V output, the chosen resistor values are 10 k Ω and 4.3 k Ω for R_{FB} and R_{PG} , respectively.

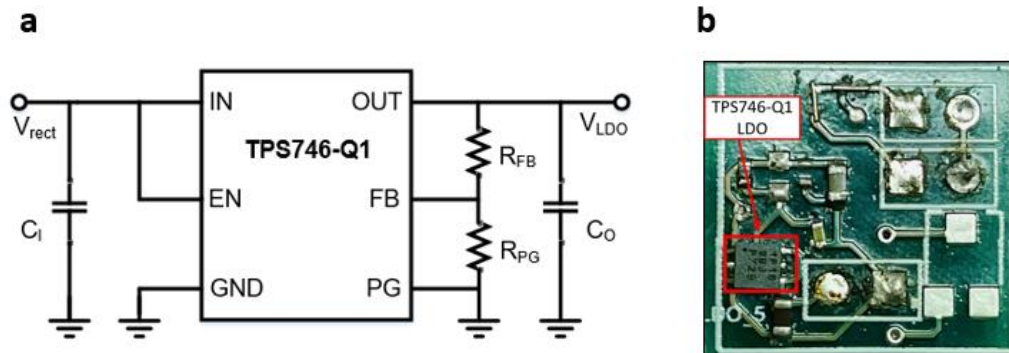


Figure 7. (a) Schematic of the TPS746-Q1 low dropout regulator. (b) PCB of the low dropout regulator.

3. RESULTS AND DISCUSSION

As mentioned earlier, the working mechanism of the high surface area REWOD energy harvester is the generation of AC voltage through periodically changing electrode-electrolyte interfacial area from an externally applied mechanical force, the pulsating pressure. AC voltages for the electrode are measured for a frequency range of 1-5 Hz with 0.5 Hz step size using an oscilloscope (Keysight InfiniiVision DSOX3014A) while applying 2.8 kPa of experimentally determined peak pulsating pressure. AC peak-to-peak voltage ranged from 1.57-3.32 V for the given frequency range. Figure 8(a) shows a linear fit peak-to-peak voltage for the 38 μm diameter pore electrode for the frequency range of 1-5 Hz with 0.5 Hz step. The AC voltage increases approximately linearly with frequency. Coefficient of determination (R^2 value) and slope from the plot in Figure 8(a) were determined to be 0.99 and 0.47 respectively showing a linear regression of AC voltage with increasing frequency. A representative plot of measured AC voltage vs. time over a 3-second time period for the 38 μm pore size electrode at 3.0 Hz is shown in Figure 8(b). The DC offset (difference between the maximum positive and negative peak) of 0.14 V and an amplitude of 2.36 V were measured from the data in the plot. The magnitude of the voltage from this work is significant realizing that no bias voltage has been applied in the experiment.

The generated charge in the REWOD electrodes is converted into the proportional voltage in the charge amplifier. The signal is digitized in the built-in microcontroller with a reference voltage of 1.65 V. The digitized signal is then transmitted through the transceiver and ceramic antenna. The transmission data rate used in this work is 250 ksamples/s. After the remote receiver receives the digitized motion signal, it is reconstructed back into analog signal in LabVIEW GUI (digital-to-analog converter). A representative signal of the motion data at 3 Hz oscillation frequency for the first 3 seconds is presented in Figure 9, which shows the reconstructed signal after the motion data is sent wirelessly to the remote receiver.

In parallel with the charge amplifier, the AC energy harvested by the REWOD system is rectified using the proposed voltage multiplier circuit. As shown in Figure 10(a), the input voltage peak-to-peak denotes the harvested AC voltage for the frequency range of 1-5 Hz with a step size of 0.5 Hz. For the lowest harvested AC voltage of 1.52 V at 1 Hz, the voltage multiplier is able to provide an output DC voltage of 3.6 V and for the highest input voltage of 3.3 V at 5 Hz frequency, the output DC voltage of the voltage multiplier is found to be 3.99 V. The maximum power conversion efficiency (PCE) is calculated to be 21% for 1 Hz frequency. The rectified DC voltage of the respective frequency is then used as the input of the LDO circuit, which is designed to provide a constant 3.3 V as output. As shown in Figure 10(b), the output voltage V_{LDO} , shows a constant voltage of 3.3 V when the LDO input voltage is above 3.3 V. For 1 Hz frequency, the system

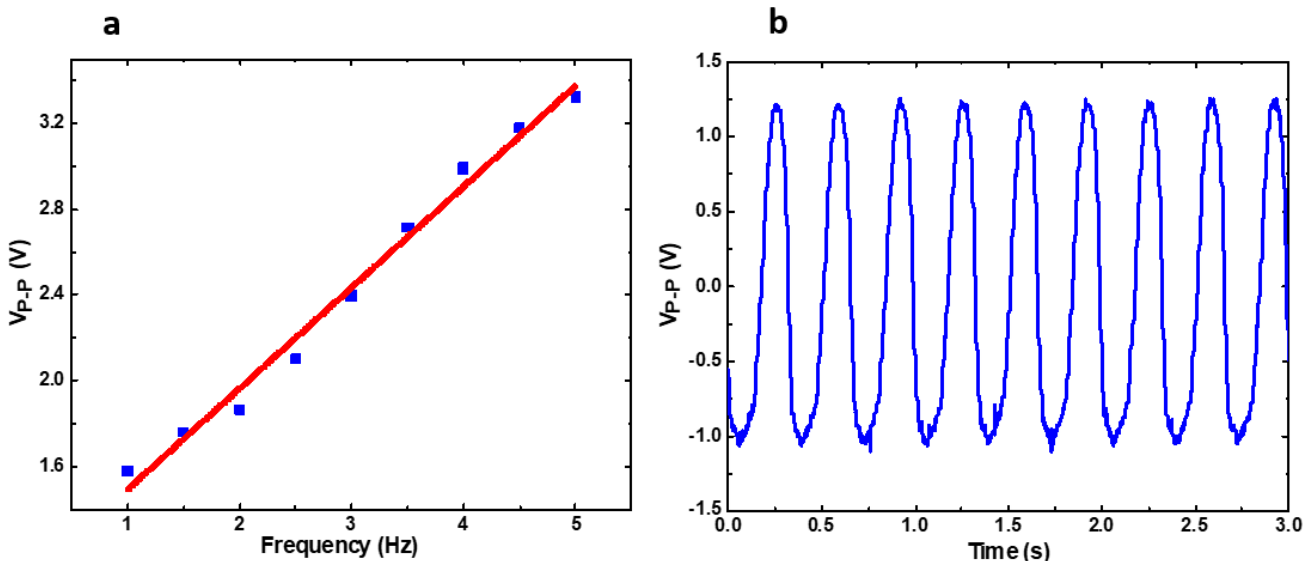


Figure 8. (a) A linear fit AC voltage for a 38 μm diameter pore electrode for a frequency range of 1-5 Hz with 0.5 Hz step. (b) A representative time scale AC voltage signal for the first 3 seconds of pulsation.

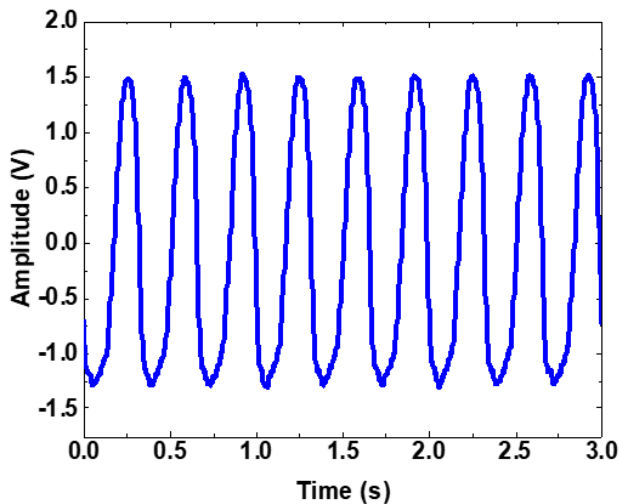


Figure 9. Reconstructed amplified AC voltage output.

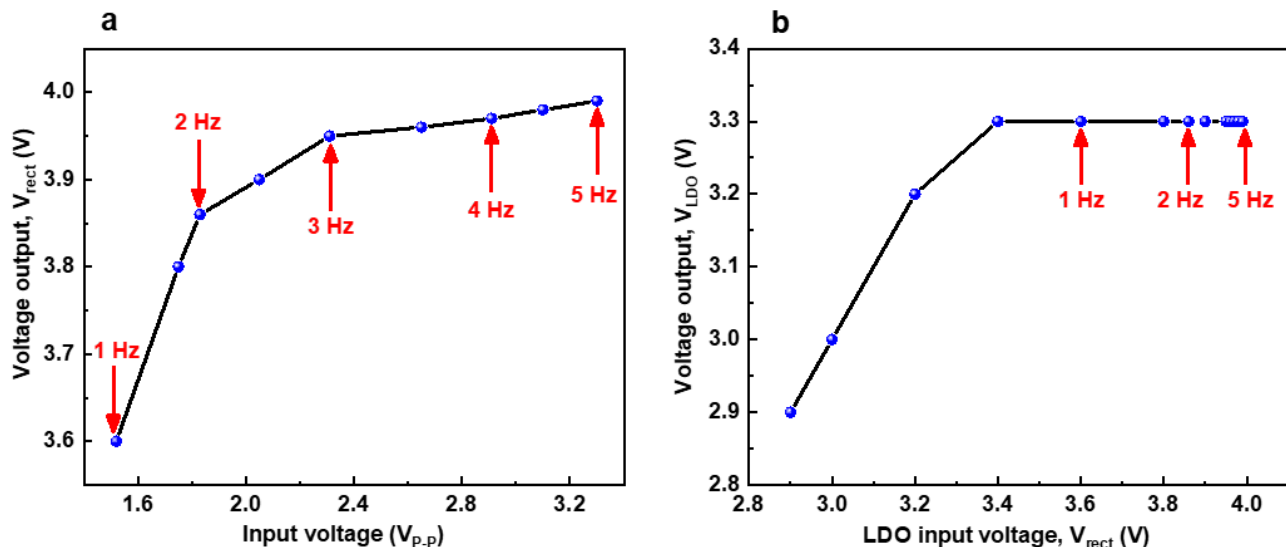


Figure 10. (a) Output voltage of the voltage multiplier for different REWOD harvested voltage for frequency range of 1-5 Hz with 0.5 Hz step size. (b) Output voltage of the LDO for different rectified voltage with 1-5 Hz frequency.

achieves the lowest harvested energy resulting in the lowest rectified voltage of 3.6 V which can still provide 3.3 V at the output of the LDO circuit. The total DC power provided by the system is approximately 1 mW for 3.3 V output voltage and 327 μ A output current.

4. CONCLUSION

In this work, REWOD-based high surface area energy harvesting was implemented using a perforated high surface area porous silicon wafer electrode with 51,784 pores, each with a diameter of 38 μ m within a circular area of 3.14 cm^2 and without application of the bias voltage. Generated AC voltage due to the continuous charging and discharging of the

electrodes was measured with respect to varying frequency. The AC voltage generation from the REWOD in the oscillation frequency range of 1-5 Hz with 0.5 Hz step size were in the range of ~1.58-3.32 V. This range of frequency aligns very well with various human motion activities such that the REWOD energy harvested from human motion could potentially power WIEs without requiring an external energy source. The DC output voltage from the multiplier for the range of AC voltage from REWOD was measured in the range of 3.6-3.99 V. In the future, a single unit device comprised of the REWOD energy harvester and the components for power conditioning and amplification could be integrated together and worn on an arm, an ankle, or a knee, etc. for motion sensing to detect whether a person is at rest, walking, or running as part of human health monitoring in real time.

5. ACKNOWLEDGEMENTS

This work is based upon work supported by the National Science Foundation (NSF) under **Grant No. ECCS 1933502**. This work was performed in part at the University of North Texas's Materials Research Facility, a shared research facility for multi-dimensional fabrication and characterization. Brian Baker at the University of Utah Nanofab is also appreciated for his assistance during electrodes fabrication process.

REFERENCES

- [1] Song, Y., Min, J., and Gao, W., "Wearable and implantable electronics: moving toward precision therapy," *ACS Nano*, 13 (11), 12280-12286 (2019).
- [2] Liu, Z., Li, H., Shi, B., Fan, Y., Wang, Z. L., and Li, Z., "Wearable and implantable triboelectric nanogenerators," *Adv. Funct. Mater.*, 29 (20), 1808820 (2019).
- [3] Hong, Y. J., Jeong, H., Cho, K. W., Lu, N., and Kim, D.-H., "Wearable and implantable devices for cardiovascular healthcare: from monitoring to therapy based on flexible and stretchable electronics," *Adv. Funct. Mater.*, 29 (19), 1808247 (2019).
- [4] Zheng *et al.*, "Robust multilayered encapsulation for high-performance triboelectric nanogenerator in harsh environment," *ACS Appl. Mater. Interfaces*, 8 (40), 26697-26703 (2016).
- [5] Won *et al.*, "Flexible vibrational energy harvesting devices using strain-engineered perovskite piezoelectric thin films," *Nano Energy*, 55, 182-192 (2019).
- [6] Guan, M., Wang, K., Xu, D., and Liao, W.-H., "Design and experimental investigation of a low-voltage thermoelectric energy harvesting system for wireless sensor nodes," *Energy Convers. Manag.*, 138, 30-37 (2017).
- [7] Toprak, A., and Tigli, O., "Piezoelectric energy harvesting: State-of-the-art and challenges," *Appl. Phys. Rev.*, 1 (3), 031104 (2014).
- [8] Wang, D.-A., and Chang, K.-H., "Electromagnetic energy harvesting from flow induced vibration," *Microelectron. J.*, 41 (6), 356-364 (2010).
- [9] Krupenkin, T., and Taylor, J. A., "Reverse electrowetting as a new approach to high-power energy harvesting," *Nat. Commun.*, 2 (1), 448 (2011).
- [10] Pachi, A. and Ji, T., "Frequency and velocity of people walking," *Struct. Eng.*, 83 (3), (2005).
- [11] Garcí-Sánchez, P. and Mugele, F., "Fundamentals of electrowetting and applications in microsystems," in *Electrokinetics and Electrohydrodynamics in Microsystems*, A. Ramos, Ed. Vienna: Springer, 85-125 (2011).
- [12] Adhikari, P. R., Tasneem, N. T., Reid, R. C., and Mahbub, I., "Electrode and electrolyte configurations for low frequency motion energy harvesting based on reverse electrowetting," *Sci. Rep.*, 11 (1), 5030 (2021).
- [13] Yang, H., Hong, S., Koo, B., Lee, D., and Y.-B. Kim, "High-performance reverse electrowetting energy harvesting using atomic-layer-deposited dielectric film," *Nano Energy*, 31, 450-455 (2017).
- [14] Yang, H., Lee, H., Lim, Y., Christy, M., and Kim, Y. B., "Laminated structure of Al₂O₃ and TiO₂ for enhancing performance of reverse electrowetting-on-dielectric energy harvesting," *Int. J. Precis. Eng. Manuf. - Green Technol.*, (2019).
- [15] Hsu, T.-H., Taylor, J. A., and Krupenkin, T. N., "Energy harvesting from aperiodic low-frequency motion using reverse electrowetting," *Faraday Discuss.*, 199 (0), 377-392 (2017).

- [16] Tricoli, A., Nasiri, N., and De, S., "Wearable and miniaturized sensor technologies for personalized and preventive medicine," *Adv. Funct. Mater.*, 27 (15), 1605271 (2017).
- [17] Carminati, M., Sinha, G. R., Mohdiwale, S., and Ullo, S. L., "Miniaturized pervasive sensors for indoor health monitoring in smart cities," *Smart Cities*, 4 (1), 146-155 (2021).
- [18] Adhikari, P. R., Tasneem, N. T., Biswas, D. K., Reid, R. C., and Mahbub, I., "Reverse electrowetting-on-dielectric energy harvesting integrated with charge amplifier and rectifier for self-powered motion sensors," *ASME 2020 Int. Mech. Eng. Congr. Expo.*, (2020).
- [19] Yang, B., Yi, Z., Tang, G., and Liu, J., "A gullwing-structured piezoelectric rotational energy harvester for low frequency energy scavenging," *Appl. Phys. Lett.*, 115 (6), 063901 (2019).
- [20] Bassett, D. R., "Validity of four motion sensors in measuring moderate intensity physical activity," *Med. Sci. Sports Exerc.*, 32 (9), S471 (2000).
- [21] Alnasser, E., "A novel low output offset voltage charge amplifier for piezoelectric sensors," *IEEE Sens. J.*, 20 (10), 5360-5367 (2020).
- [22] Tasneem, N. T., Biswas, D. K., Adhikari, P. R., Reid, R., and Mahbub, I., "Design of a reverse-electrowetting transducer based wireless self-powered motion sensor," in *2020 IEEE International Symposium on Circuits and Systems (ISCAS)*, 1-5 (2020).
- [23] Perera, T., Yohanandan, S. A. C., and McDermott, H. J., "A simple and inexpensive test-rig for evaluating the performance of motion sensors used in movement disorders research," *Med. Biol. Eng. Comput.*, 54 (2-3), 333-339 (2016).
- [24] Litwhiler, D. H., "A custom vibration test fixture using a subwoofer," 11 (2011).
- [25] Han, K., Woghiren, O. E., and Priefer, R., "Surface tension examination of various liquid oral, nasal, and ophthalmic dosage forms," *Chem. Cent. J.*, 10, (2016).
- [26] Analog Devices Datasheet, "ADA4691-2 Low Power, 3.6 MHz, Low Noise, Rail-to-Rail Output, Operational Amplifiers."
- [27] Texas Instrument Datasheet, "CC430F5137 16-Bit ultra-low-power CC430 Sub 1 GHz wireless MCU with 12-Bit ADC, 32kB Flash and 4kB RAMCC430F5137.
- [28] Park, S., Yang, J., and Rivas-Davila, J., "A Hybrid Cockcroft-Walton-Dickson multiplier for high voltage generation," *IEEE Trans. Power Electron.*, 35 (3), 2714-2723 (2020).
- [29] Texas Instrument Datasheet, "TPS61220 Low Input Voltage, 0.7V Boost Converter with 5.5 μ A Quiescent Current".